JVST A
Journal of Vacuum Science & Technology A

ARTICLE

avs.scitation.org/journal/jva

Area-selective molecular layer deposition of nylon 6,2 polyamide: Growth on carbon and inhibition on silica

Cite as: J. Vac. Sci. Technol. A 39, 023204 (2021); doi: 10.1116/6.0000769
Submitted: 9 November 2020 · Accepted: 13 January 2021 ·
Published Online: 11 February 2021

Marcel Junige and Steven M. George

AFFILIATIONS

Department of Chemistry, University of Colorado, 215 UCB, Boulder, Colorado 80309-0215

Note: This paper is a part of the Special Topic Collection on Area Selective Deposition.

ABSTRACT

In microelectronic or nanoelectronic manufacturing, pattern transfer by directional reactive ion etching (RIE) progressively erodes amorphous carbon (aC) hard masks. To maintain critical dimensions and tolerances of high-aspect-ratio device structures, new carbonaceous materials may be added repeatedly to replace the eroded aC hard mask. Such a mask repairing step during RIE needs self-aligning growth of organic materials. Area selectivity is required to deposit the organic material on the aC hard mask exclusively. Deposition on the dielectric or semiconductor device structures underlying the mask would complicate their precise etching or later cleaning. When ashing the aC hard mask, all-organic materials are preferable to organic-inorganic hybrid materials because they leave no residue. In this work, area-selective molecular layer deposition (MLD) was developed for the all-organic polyamide nylon 6,2. The monomer reactants for nylon 6,2 MLD were ethylene diamine and adipoyl chloride. Nylon 6,2 MLD was studied in the homogeneous, steady-state growth regime and during nucleation on various starting surfaces utilizing *in situ* spectroscopic ellipsometry. Area-selective MLD of nylon 6,2 was achieved on the "growth" carbon surface in the presence of silica by functionalizing aC via mild oxidation. In addition, a surface passivant was selectively attached to silica by using an amine-catalyzed coupling chemistry. The passivant inhibited the nylon 6,2 MLD on the "nongrowth" silica surface. A single passivation pretreatment was sufficient to restrict the MLD on the silica surface. The passivant, however, did not substantially impact the MLD nucleation and growth on the aC surface. This strategy yielded area selectivity with exceptionally high quality and over a wide range of MLD cycles. The area-selective MLD of nylon 6,2 was further applied on industrial test features with aC patterns masking trenches in silica. This demonstration illustrated the capability of area-selective MLD to repair RIE-eroded aC hard masks and to maintain the critical dimension.

I. INTRODUCTION

State-of-the-art production of integrated circuits has reached the 5 nm node with physical minimum feature sizes around 10 nm.[1,2] This shrinking will continue to progress and has demanded novel approaches for deposition, patterning, and etching.[3–6] At present, critical dimensions (CDs) need to be maintained within tolerances of 1 nm or less.[6,7] The CD can be the width of, or the pitch between, two dual-damascene interconnect trenches[8] or vertical-interconnect-access holes.[9,10] The placement, shape, and size of such complex device structures have traditionally been implemented through masks.[11–13] Reactive ion etching (RIE) has been used for highly directional, anisotropic material removal to transfer the mask patterns into semiconductor or dielectric materials.[14,15]

With continually miniaturized feature sizes, as well as increasingly demanding three-dimensional shapes, photoresists alone have become too thin for pattern transfer using RIE. For instance, a photoresist for sub-22 nm lithography would not withstand high-energy ion bombardment and would erode quickly during RIE. Trilayer mask stacks employing amorphous carbon (aC) have been introduced to solve this challenge.[16–19] The corresponding processing sequence is illustrated in Fig. 1: First, photoresist is patterned by photolithography. A thin silicon (Si)-based film underneath the photoresist serves as antireflective coating. The patterns in the photoresist then mask the etching of the Si-based film. Subsequently, this Si-based mask is used for etching into a thicker aC film. This aC hard mask allows for precise pattern transfer into the underlying semiconductor or dielectric.

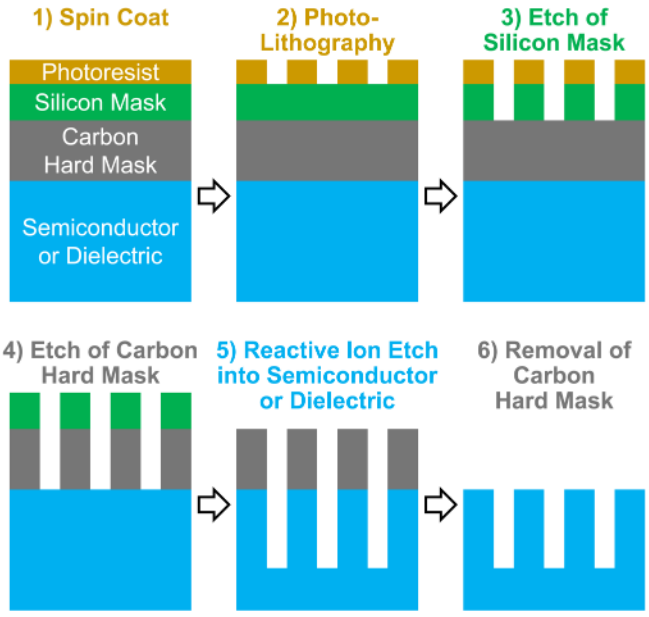

FIG. 1. Processing sequence to manufacture high-aspect-ratio device structures using trilayer mask stack for RIE into semiconductor or dielectric. Photoresist is used to pattern the silicon mask. Silicon mask is used to pattern the carbon hard mask prior to RIE into the underlying substrate.

Inconveniently, when driving ever smaller device structures deeper into more and more challenging aspect ratios, RIE can progressively erode even the aC hard mask.[20] This problem will become more pressing with each future technology node.[1–7] As a potential solution, the focus of the present study was to develop a technique to repair the aC hard mask during RIE. The goal was to add new carbonaceous material compensating for the aC erosion by RIE to maintain the CD. Area-selective molecular layer deposition (MLD) was developed to coat an organic polymer on the aC hard mask exclusively. No MLD on the semiconductor or dielectric device structures was desired because this MLD would complicate the precise etching or cleanliness of these structures. In this way, the area-selective MLD approach was advantageous compared with the BOSCH deep RIE process.[15]

When eventually removing the aC hard mask by ashing, all-organic polymers are preferable to organic-inorganic hybrids. The inorganic component in hybrid organic-inorganic MLD films leaves behind an inorganic residue after ashing. In contrast, all-organic polymers can be ashed without leaving a residue. MLD processes of various all-organic polyamide films and other all-organic polyimide and polyurea films have been developed previously.[21–26]

Area-selective MLD of polyimide has recently been reported on copper versus native silicon dioxide.[27] Moderate, inherent selectivity without the use of a passivant has been found at an optimal temperature of 200–210 °C. In addition, polyurea MLD has been deposited selectively on metal-dielectric patterns using self-assembled monolayers (SAMs) to block the metal areas.[28–31] However, selectivity was lost after 6 nm of polyurea MLD growth on the dielectric and defects in the SAMs necessitated additional correction steps.[30,31] Consequently, innovating more robust blocking layers that can withstand a larger number of MLD cycles is essential.

In this study, area-selective MLD of all-organic nylon 6,2 polyamide was achieved with nucleation and growth on mildly oxidized aC but inhibition on passivated silica (SiO_2). At least 16 nm of nylon 6,2 MLD was obtained on the aC "growth" surface with exceptionally high selectivity above 98% in comparison to the passivated SiO_2 "nongrowth" surface. The high selectivity remained for at least 100 MLD cycles after a single surface passivation treatment. This excellent selectivity was further transferred to industrial test features containing both aC and SiO_2 areas in proximity as verified by scanning electron microscopy (SEM).

II. EXPERIMENT

The area-selective MLD experiments presented here were conducted in a hot-wall, viscous-flow vacuum reactor. The MLD reactor design was inspired by earlier hot-wall, viscous-flow atomic layer deposition (ALD) reactors.[32] The reactor tube incorporated a V-shape to enable *in situ* spectroscopic ellipsometry (iSE) at an angle of incidence of 70°. This reactor featured a small gas volume, laminar gas flow conditions, and isothermal heating. The reactor walls and sample surface were nearly at the same temperature. The base pressure was 10 mTorr after evacuation with a dual-stage mechanical pump (Pascal 2010 C1, Pfeiffer Vacuum GmbH). The reactor walls and sample holder were cleaned from polymer deposits after every MLD experiment by etching with a continuous flow of ozone (O_3) for at least 2 h. A fresh sample was loaded after reactor cleaning.

The monomer reactants for nylon 6,2 MLD were ethylene diamine (ED, ≥99% purity from Sigma Aldrich, 10 Torr vapor pressure at 20 °C) and adipoyl chloride (AC, 98% purity from Sigma Aldrich, 2 Torr vapor pressure at 20 °C). Similar polyamide MLD films have been deposited earlier using different diamine and diacid chloride precursors.[21–24] ED and AC were exposed by three microdoses in the vapor draw mode. The reactor was evacuated for 45 s before drawing the ED and AC vapor for 1 and 1.5 s, respectively, from a stainless-steel cylinder. The second and third microdoses were each drawn after a 15 s reload period. The reactor remained connected to the pump during vapor draw. This ensured evacuation of the hydrogen chloride by-product. ED was kept at room temperature. AC was heated to 70 °C. Typical ED exposures were 600 mTorr s at a vapor draw pressure of 200 mTorr. Typical AC exposures were ~30 mTorr s at a vapor draw pressure of ~7 mTorr. Sequential monomer exposures were separated by respective purge steps using inert argon (Ar, 99.998% purity from Airgas) gas in viscous flow at 1 Torr for 120 s.

To achieve area selectivity, favorable chemistry was needed between one of the MLD reactants and the aC surface ("growth" area). In addition, unfavorable chemistry was needed between both the MLD reactants and the SiO_2 surface ("nongrowth" area). This selectivity was achieved by pretreating the two distinct starting surfaces as illustrated in Fig. 2.

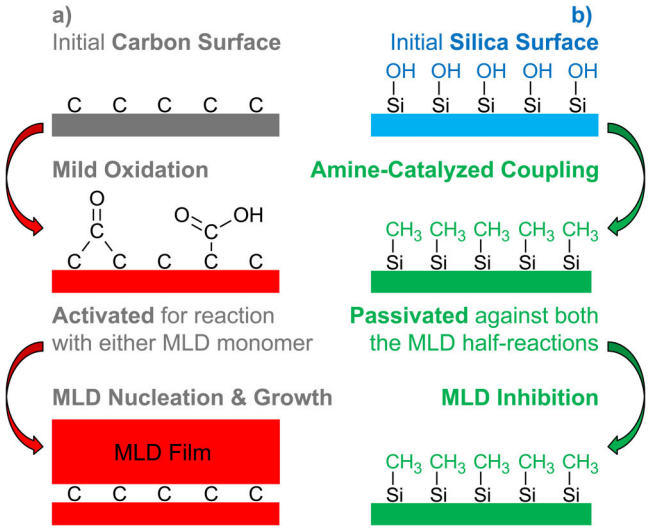

FIG. 2. Preparation of initial surfaces for area-selective MLD: (a) Activation of aC for reaction with either MLD monomer by mild oxidation. (b) Passivation of hydroxylated SiO_2 against polymer MLD by amine-catalyzed coupling of methylated silane.

The initial aC surface was mildly oxidized as shown in Fig. 2(a) using a 50 wt. % solution of H_2O_2 (hydrogen peroxide) in water (with proprietary tin-based stabilizer from Sigma Aldrich, 23 Torr vapor pressure at 30 °C). H_2O_2 is preferable to O_3 because O_3 can spontaneously etch aC films at a high etch rate. H_2O_2 was exposed using 50 doses in the static mode. During this static mode dosing, the reactor was evacuated for 45 s before closing a gate valve between the reactor and the pump. Subsequently, H_2O_2 vapor was drawn for 1 s from a glass flask kept at room temperature. After 30 s of static exposure, the gate valve was opened, reconnecting the reactor to the vacuum pump. Each H_2O_2 exposure yielded 135 Torr s at a static pressure of 4.5 Torr. This mild H_2O_2 oxidation activated the initial aC surface for reaction with the MLD monomers. Although H_2O_2 was used, the aC surface was also oxidized and activated by exposure to ambient air.

The initial SiO_2 surface was cleaned using 50 static doses of H_2O_2 and then passivated against polymer MLD nucleation using amine-catalyzed coupling chemistry[33–37] as shown in Fig. 2(b). O_3 was not used to clean the initial SiO_2 surface because O_3 could dehydroxylate the SiO_2 surface and produce siloxane bridges. Ten static doses of dimethylaminotrimethylsilane (DMA-TMS, 97% purity from Sigma Aldrich, 67 Torr vapor pressure at 25 °C) were used for passivation of the SiO_2 surface. Each static DMA-TMS dose was conducted at a pressure of 7 Torr for 30 s to yield a DMA-TMS exposure of 210 Torr s. DMA-TMS was kept in a stainless-steel cylinder at room temperature. DMA-TMS has been reported to chemisorb selectively on hydroxylated SiO_2.[38] This catalyzed coupling capped the SiO_2 surface with methyl groups from $-Si(CH_3)_3$ surface species and passivated against polymer MLD.

Industry-standard aC films currently used for advanced lithography and etch patterning were provided by Tokyo Electron (TEL) on 300 mm wafers. These aC films were deposited using plasma-enhanced chemical vapor deposition. TEL also provided 300 mm wafers with three-dimensional test features consisting of trenches in SiO_2 fabricated by RIE through aC hard mask patterns. MLD experiments were conducted on these wafer samples hand-diced into 0.5×0.5 in.^{2} coupons.

Simulations were performed to determine the sensitivity of iSE to the MLD polymer growth on aC samples. To optimize the sensitivity, a transparent SiO_2 interlayer was inserted in the optical sample structure between the Si wafer and aC hard mask. This SiO_2 interlayer provided an interference enhancement effect.[39] Figure 3(a) shows the simulation results for the predicted signal changes in the ellipsometric angle *Psi* (on the left scale) and *Delta* (on the right scale), respectively, for incrementing MLD polymer

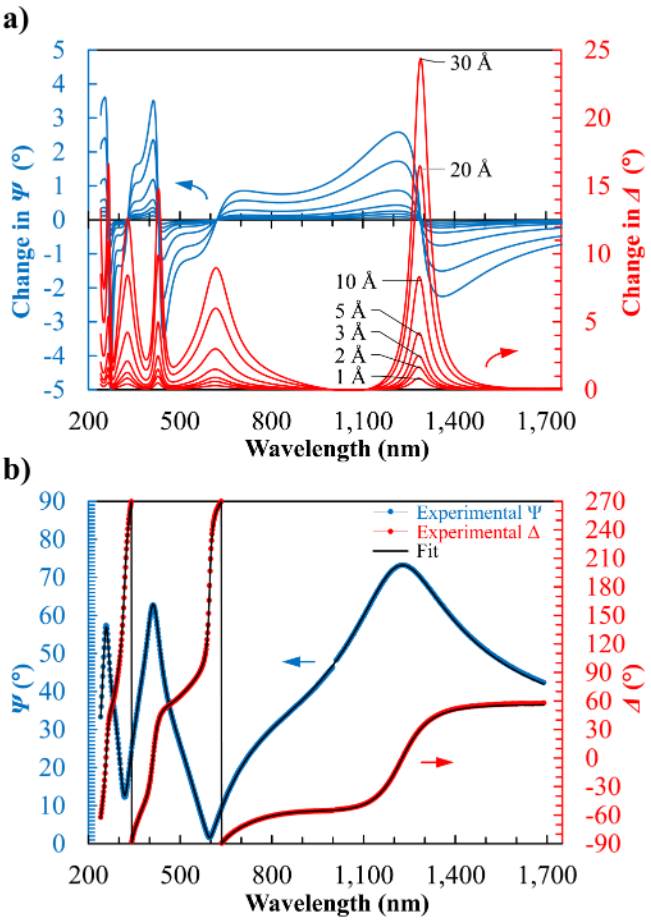

FIG. 3. (a) Projected changes in ellipsometric data (*Psi*: left scale; *Delta:* right scale) for incrementing thickness of polymer top layer based on optical simulations. (b) Ellipsometric *Psi* and *Delta* measurements of the aC film on SiO_2 interlayer on silicon wafer. Best model fit was obtained with aC thickness of ~18 nm and SiO_2 thickness of ~250 nm.

thicknesses. Each spectrum was referenced to the pristine aC sample. These simulations revealed that ~250 nm for the SiO_2 interlayer thickness and ~20 nm for the aC hard mask thickness yielded optimal sensitivity to ultrathin MLD polymer growth.

When adding 1 Å of polymer to the aC surface, Fig. 3(a) shows that the interference enhancement generated a change in *Delta* slightly above 1°. This signal gain occurred in all spectral regions: the infrared above 1000 nm, the visible, and the ultraviolet below 400 nm. Given the iSE instrumental noise in *Delta* below ±0.2°, these signal gains corresponded to a signal-to-noise ratio around 10 dB. Consequently, this sample structure provided sufficient iSE sensitivity to detect MLD polymer growth well below 1 Å. These signal gains increased with incrementing MLD polymer thicknesses.

Initial aC samples from TEL were characterized by *ex situ* variable angle spectroscopic ellipsometry utilizing an M2000 instrument by J.A. Woollam Co., Inc. Figure 3(b) shows the experimental measurement (solid circles) and the optical model adjustment (solid lines). The experimental ellipsometric raw data, *Psi* (left scale) and *Delta* (right scale), exhibited the spectral interference from the SiO_2 interlayer. After adjustment of the aC film thickness to ~18 nm, the optical model matched the experimental data. Noteworthy, double-side-polished Si wafers had to be roughened on the backside by bead-blasting with silicon carbide sand to suppress standing waves. Otherwise, Fabry–Pérot resonances resulted from the transparency of Si in the infrared spectral region.

An iSE instrument by J.A. Woollam Co., Inc., was mounted on the MLD reactor. This iSE was utilized to characterize the cleaning of initial surfaces, the passivation of SiO_2, and the nylon 6,2 MLD during both the homogeneous, steady-state growth regime and the nucleation period. The MLD nucleation on various starting surfaces was studied on individual substrates, one material at a time. Each nucleation experiment was repeated twice to check for reproducibility. Gate valves isolated the optical view ports for the iSE instrument from the reactor gas phase during reactant exposures. Ellipsometric spectra were acquired for 5 s after Ar purging at the end of each completed MLD cycle. *In situ* ellipsometry has been utilized previously to investigate the nucleation of ALD processes.[40,41]

SEM (Hitachi) was utilized at TEL for imaging of industrial test features in the CD top view[6] as well as in the cross-sectional view. These SEM images were recorded before and after applying area-selective MLD. This high-resolution SEM imaging enabled the characterization of both aC and SiO_2 areas in close proximity.

III. RESULTS AND DISCUSSION

A. MLD nucleation and growth on initial, oxidized carbon

Initial aC films provided by TEL were first cleaned and activated using 50 static doses of H_2O_2 at 125 °C. This cleaning process was monitored by iSE. The aC film thickness decreased continuously at a rate of −0.1 Å per H_2O_2 exposure during these 50 static H_2O_2 doses. This continuous loss of aC thickness was attributed to the removal of ambient contaminations, as well as a very slow, spontaneous etching of the aC hard mask. The spontaneous etching of aC was consistent with the mild oxidation of aC. Previous studies have revealed that O_3 can mildly oxidize carbon surfaces and produce carboxylic acid and/ or carbonyl surface species.[42] Earlier investigations have also concluded that gaseous carbon oxide species do not desorb from carbon surfaces until temperatures above 150 °C.[43]

Nylon 6,2 polymer MLD was then studied on the H_2O_2-oxidized aC surface. Figure 4(a) (solid triangles) shows the iSE results for the nylon 6,2 film thickness versus MLD cycle number. The nylon 6,2 film grew progressively over 100 MLD cycles at 125 °C. The nucleation was rapid over the first ten MLD cycles. The MLD growth was linear with a growth per cycle (GPC) of 1.6 Å after 60 MLD cycles.

Rapid MLD nucleation in the substrate-enhanced mode[44] indicated that the aC surface was successfully activated by H_2O_2. Reactive species, such as oxygen-containing carboxylic acid and/ or carbonyl groups, were probably present that acted as effective adsorption sites. The substrate-enhanced growth mode was consistent with a high density of these initial adsorption sites.[44] This rapid nucleation ensured that the individual polymer chains forming the nylon 6,2 film had a high density.

A closer look at the first five MLD cycles with resolution of the individual ED/AC half-reactions revealed that the nylon 6,2 thickness incremented significantly after both initial ED exposures and initial AC exposures. These immediate, significant thickness gains with each initial monomer exposure suggested that both the ED and AC monomers reacted favorably with the surface species on the activated aC surface.

B. MLD nucleation and growth on initial, hydroxylated silica

Initial SiO_2 substrates were also cleaned using 50 static doses of H_2O_2 at 125 °C. This surface cleaning was monitored by iSE. The optical thickness of a top layer decreased at a rate of −0.2 Å per H_2O_2 exposure. The thickness stabilized after a decrement of no more than 5 Å within 20–30 static H_2O_2 exposures. Although this top layer was modeled using the optical material parameters of SiO_2, the thickness loss probably resulted from a removal of adventitious carbon from the SiO_2 substrate. Direct surface analysis with techniques such as x-ray photoelectron spectroscopy might confirm the nature of the removed material. In addition, the H_2O_2 exposures were believed to leave the SiO_2 surface covered with a high density of hydroxyl groups. Preliminary water contact angle measurements were consistent with a very hydrophilic surface. Previous studies have rehydroxylated SiO_2 surfaces using water (H_2O) plasma exposures.[45]

Nylon 6,2 polymer MLD was then studied on the initial, hydroxylated SiO_2 surface. Figure 4(b) (solid diamonds) shows the iSE results for the nylon 6,2 film thickness versus MLD cycle number. The nylon 6,2 film grew progressively over 100 MLD cycles at 125 °C. Although the nucleation was slightly reduced over the first eight MLD cycles compared with the results on aC in Fig. 4(a), the MLD growth became linear with a GPC of 1.9 Å after 60 MLD cycles.

An expansion of the first five MLD cycles with half-cycle resolution revealed that the nylon 6,2 thickness did not change significantly after initial ED exposures. In contrast, the thickness incremented after every initial AC exposure. The negligible thickness gains after initial ED exposures suggested an insufficient adsorption of the ED monomer at hydroxyl groups on the SiO_2

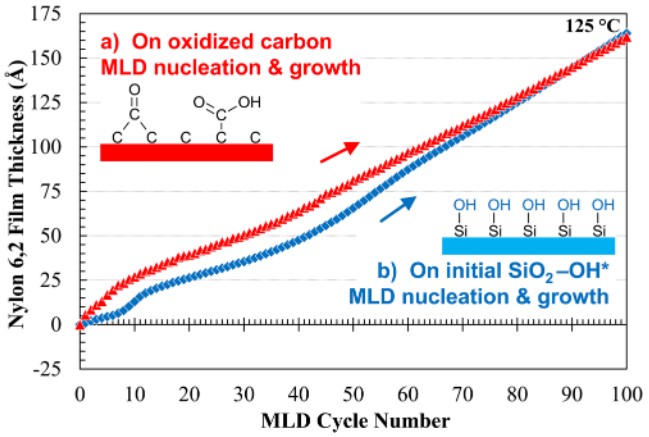

FIG. 4. Nylon 6,2 MLD film thickness derived from iSE during nylon 6,2 MLD at 125 °C (a) on initial, oxidized aC surface (triangles) and (b) on initial, hydroxylated SiO_2 surface (diamonds).

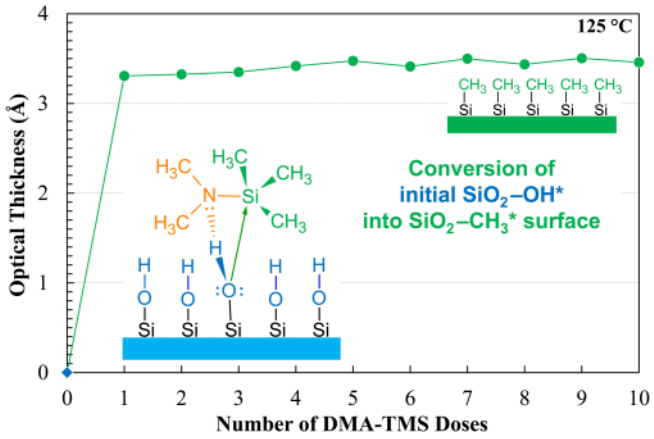

FIG. 5. Optical thickness during ten, consecutive static exposures of DMA-TMS on hydroxylated SiO_2 at 125 °C. Amine-catalyzed chemisorption of DMA-TMS converts hydroxylated SiO_2 surface to methylated SiO_2 surface.

surface. On the other hand, the significant thickness gains after the initial AC exposures suggested that hydroxyl groups on SiO_2 served as effective adsorption sites for the AC monomer.

The reduced, slower nucleation suggested the formation of a less dense nylon 6,2 MLD film on hydroxylated SiO_2 compared with the film on aC. This lower density was consistent with a lower refractive index in the ordinary direction of the uniaxial film as revealed by a multitime-slice analysis of the iSE data. The lower mass density was also confirmed by x-ray reflectivity measurements. A lower density of individual polymer chains can open a pathway for the diffusion of monomers during the homogeneous, steady-state MLD growth regime.[46,47] This monomer diffusion might explain the slightly increased GPC as compared with the growth of a denser nylon 6,2 MLD film on oxidized aC.

Nylon 6,2 MLD was able to nucleate and grow on the initial SiO_2 surface. No inherent selectivity was found for nylon 6,2 MLD between aC and SiO_2 surfaces as has been obtained for other deposition systems.[27,40,41,48,49] Consequently, passivation of the SiO_2 surface was required to achieve area-selective MLD on the aC "growth" surface but not on the SiO_2 "nongrowth" surface.

C. MLD inhibition on passivated silica

The passivation of an initial, hydroxylated SiO_2 surface after H_2O_2 cleaning was accomplished by the adsorption of DMA-TMS. Figure 5 shows the optical thickness of a layer on top of the SiO_2 surface as a function of ten, consecutive static exposures of DMA-TMS at 125 °C. This optical top layer was modeled with the material parameters of SiO_2. The thickness increased abruptly and saturated immediately at 3.4 Å after the first DMA-TMS exposure. This material addition was evident in the ellipsometric raw data as a red shift of the spectral interference patterns.

Since iSE relies on photon-electron interactions, the surface sensitivity of iSE is limited by the polarizability of surface groups. While hydroxyl groups exhibit a very low electronic polarizability due to the high electronegativity of oxygen, methyl groups are among the most polarizable.[50] Consequently, iSE is very sensitive to methyl groups on the surface. The rapid thickness gain after the first static DMA-TMS exposure was interpreted as the effective and efficient adsorption of methyl groups, presumably in the form of trimethylsilyl [$-Si(CH_3)_3$] surface species. Preliminary water contact angle measurements were consistent with a very hydrophobic surface.

The successful adsorption of DMA-TMS was expected from the amine-catalyzed coupling chemistry. Earlier work has shown that pyridine or ammonia as an amine can catalyze SiO_2 ALD using tetrachlorosilane or tetraethoxysilane and water as reactants at low temperatures between 17 and 102 °C.[33–37] The amine catalysis is based on Si-OH surface species having a very acidic hydrogen with an isoelectric point at pH = 2.[51] Amine coupling to this Si-OH* hydrogen makes the oxygen in Si-OH* a much stronger nucleophile for reaction with chlorosilanes and aminosilanes.[33]

The present study used DMA-TMS as the silane that contains the amine catalyst in itself. This concept has been described as "self-catalysis."[52,53] The reaction of DMA-TMS vapor with Si-OH surface species produces $SiO\text{-}Si(CH_3)_3$ surface species and volatile dimethylamine (DMAH). DMAH can further catalyze the attachment of DMA-TMS. An earlier study has reported using DMA-TMS for passivation of SiO_2 against the ALD of noble metals although this work mainly utilized bisdimethylaminodimethylsilane.[38] Possible alternative silanes for the passivation of hydroxylated SiO_2 include tridecafluoro-1,1,2,2-tetrahydrooctyl-methylbis(dimethylamino) silane[54] or trimethylchlorosilane. Note that chlorosilanes require an amine catalyst.[33]

The SiO_2 surface covered with $-Si(CH_3)_3$ species after DMA-TMS adsorption was expected to be returned to a hydroxylated SiO_2 surface after exposure to oxidizing agents. Subsequently, DMA-TMS adsorption could again form a new surface passivation layer. The methylated SiO_2 surface should be stable under vacuum conditions at temperatures up to 300 °C.[54]

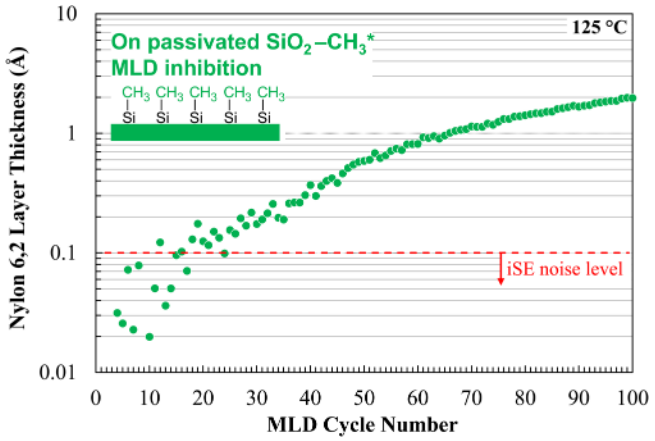

FIG. 6. Nylon 6,2 MLD film thickness derived from iSE during nylon 6,2 MLD on methylated SiO_2 surface after passivation with DMA-TMS at 125 °C. MLD was greatly inhibited for at least 100 MLD cycles.

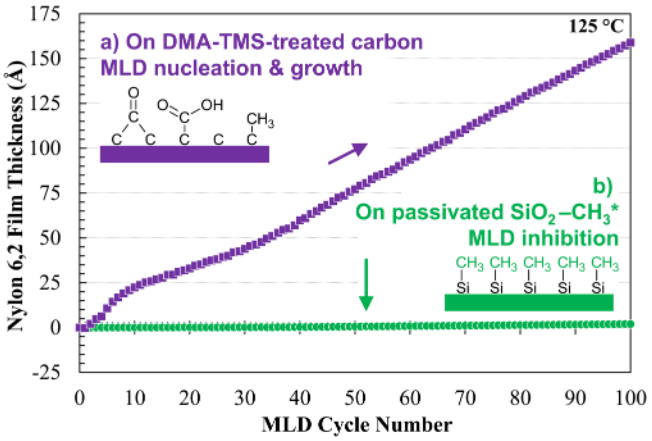

FIG. 7. Nylon 6,2 film thickness derived from iSE during nylon 6,2 MLD at 125 °C (a) on aC surface after DMA-TMS pretreatment (squares) and (b) on methylated SiO_2 surface after DMA-TMS passivation (circles). MLD nucleated and grew on aC surface exclusively but was inhibited on passivated SiO_2 surface.

Nylon 6,2 polymer MLD was then studied on the SiO_2 surface passivated by DMA-TMS. Figure 6 shows the iSE results for the nylon 6,2 layer thickness on a logarithmic scale versus the MLD cycle number at 125 °C. No significant polymer MLD was observed on the passivated SiO_2 surface. The nylon 6,2 thickness remained below the iSE noise level of 0.1 Å during the initial 20 MLD cycles and stayed below 1 Å for 65 MLD cycles. The nylon 6,2 thickness was less than 2 Å after 100 MLD cycles.

The results in Fig. 6 indicated that the nylon 6,2 MLD nucleation was strongly inhibited on the passivated SiO_2 surface. The SiO_2 surface methylated with $–Si(CH_3)_3$ species after DMA-TMS adsorption was unfavorable for nylon 6,2 polymer MLD. This substrate-inhibited nucleation has been assigned to an island growth mode.[41,44,55] No closed nylon 6,2 film formed on the passivated SiO_2 surface. Instead, only a few isolated polymer chains were assumed to grow scattered across the surface. Direct imaging techniques such as atomic force microscopy might reveal the morphology and surface coverage of the scattered polymer islands. When applying hundreds of more MLD cycles, these scattered polymer deposits may eventually grow together and lead to much increased MLD film growth.

D. MLD nucleation and growth on carbon after passivation of silica

In practical use, the DMA-TMS treatment employed to passivate the SiO_2 surface will equally encounter the aC surface. For area-selective polymer MLD, DMA-TMS exposures must not affect the MLD nucleation and growth on the aC surface. To determine if aC was modified by the passivation treatment, the aC surface was exposed to 50 static doses of H_2O_2 and then to the same 10, consecutive static doses of DMA-TMS at 125 °C. After this procedure, Fig. 7(a) (solid squares) displays the nylon 6,2 film thickness for 100 MLD cycles at 125 °C.

In similarity with the results on oxidized aC in Fig. 4(a), the very first and each following MLD cycle yielded significant thickness gains. The thickness gain per cycle was slightly higher for the initial eight cycles than for the subsequent MLD cycles. The nylon 6,2 MLD film grew with a linear GPC of 1.7 Å after 60 MLD cycles. The DMA-TMS treatment had negligible impact on the nylon 6,2 polymer MLD on the aC surface. These results argued that DMA-TMS did not react with the oxidized aC surface. The amine catalysis requires the very acidic Si-OH surface species on hydroxylated SiO_2.[33,51]

The passivation of SiO_2 was performed with little consequence to the aC surface. Figure 7(b) (solid circles) shows the iSE results for nylon 6,2 MLD on the passivated SiO_2 surface from Fig. 6 in the same diagram as the nylon 6,2 MLD on the aC surface subjected to the DMA-TMS pretreatment. This comparison highlights the dramatic difference between these two surfaces. MLD nucleation and growth obtained at least 16 nm of nylon 6,2 on the aC surface. At the same time, greatly restricted "nongrowth" was accomplished on the passivated SiO_2 surface.

E. Selectivity index

To quantify area selectivity, a selectivity index has been defined according to the following expression:[56–58]

$$\text{Selectivity Index} = \left(1 - \frac{\text{Thickness on "Nongrowth" Surface, i.e., Silica}}{\text{Thickness on "Growth" Surface, i.e., Carbon}}\right) \cdot 100\%. \quad (1)$$

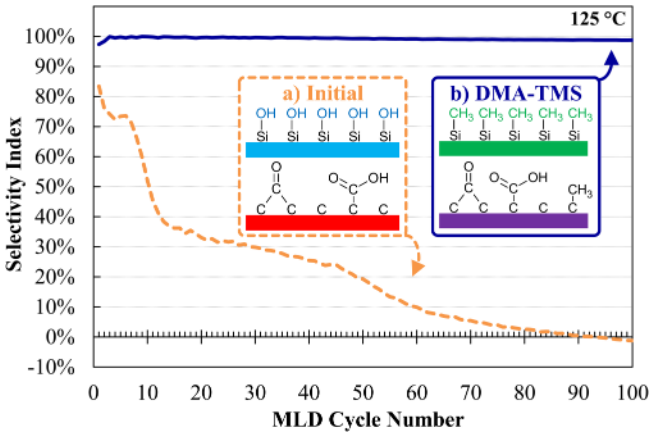

FIG. 8. Selectivity index over 100 cycles of nylon 6,2 MLD at 125 °C (a) for initial, oxidized aC surface vs initial, hydroxylated SiO_2 surface (dashed line) and (b) for DMA-TMS-treated aC surface vs DMA-TMS-passivated SiO_2 surface (solid line). After DMA-TMS pretreatment, selectivity was >98% for at least 100 MLD cycles.

The value of the selectivity index ranges from 0% to 100%. Zero signifies no selectivity due to equal thickness gains on both the "growth" and "nongrowth" surface areas. 100% defines ideal selectivity with full blockage of the "nongrowth" surface area and a thickness gain exclusively on the "growth" surface area. This equation was used to determine the selectivity index for the aC surface versus the SiO_2 surface over 100 MLD cycles.

Figure 8(a) (dashed line) shows the selectivity index for the initial, H_2O_2-oxidized aC surface versus the initial, H_2O_2-hydroxylated SiO_2 surface, based on the nylon 6,2 film thicknesses in Fig. 4. This selectivity index started at around 80% and then fell below 50% within the first ten MLD cycles. The selectivity index decreased further to zero with increasing number of MLD cycles. In contrast, Fig. 8(b) (solid line) shows the selectivity index for the DMA-TMS-treated aC surface versus the DMA-TMS-passivated SiO_2 surface, based on the nylon 6,2 film thicknesses in Fig. 7. This selectivity index remained above 98% for all 100 MLD cycles. This high selectivity confirmed the excellent passivation of the SiO_2 surface using selective adsorption of DMA-TMS.

Even higher selectivity over more MLD cycles could be obtained using a mild etching step to remove the minor polymer deposits from the SiO_2 surface. This procedure has been utilized in other deposition systems to enhance area selectivity.[59–64] A mild etching of polymers could be performed using either O_3 or H_2O_2. O_3 and H_2O_2 exposures on nylon 6,2 MLD films were observed to etch the all-organic films at moderate rates. This etching left no residues detectable by iSE after complete removal of the nylon 6,2 MLD films. Etching with H_2O_2 exhibited a slightly lower rate but might be preferable for terminating the SiO_2 surface with hydroxyl groups. Hydroxyl groups on SiO_2 are essential for the attachment of the DMA-TMS passivant.

F. Area-selective MLD of nylon 6,2 on three-dimensional test features

The above surface pretreatments and nylon 6,2 MLD were applied on three-dimensional test features to confirm the area selectivity observed on planar substrates. These test features were fabricated by TEL using an industrial RIE process to etch trench structures into SiO_2 through aC hard mask patterns.

Figure 9(a) displays a cross-sectional SEM micrograph of the initial sample showing the aC lines and the underlying SiO_2 substrate with trenches etched by RIE. The aC hard mask was ~500 nm in height. The nominal line width and pitch were 200 and 400 nm, respectively. The RIE process eroded the aC patterns into narrower lines with a conical shape at the top. This aC hard mask erosion induced an error in the CD line width. In addition, RIE appeared to have sputtered and redeposited some SiO_2 on the sidewalls of the aC lines. The bright intensity of the sidewalls in Fig. 9(a) was consistent with the charging of an electrically

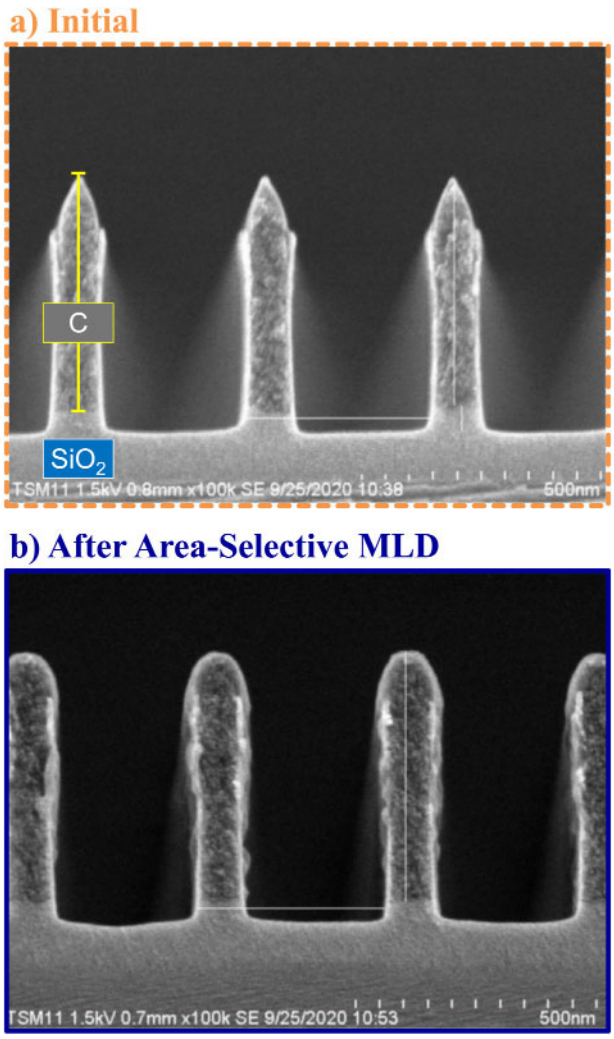

FIG. 9. Cross-sectional SEM image of (a) aC hard mask patterns (lines) used to etch trench structures into underlying SiO_2 substrate by RIE and (b) same test features after area-selective MLD of nylon 6,2.

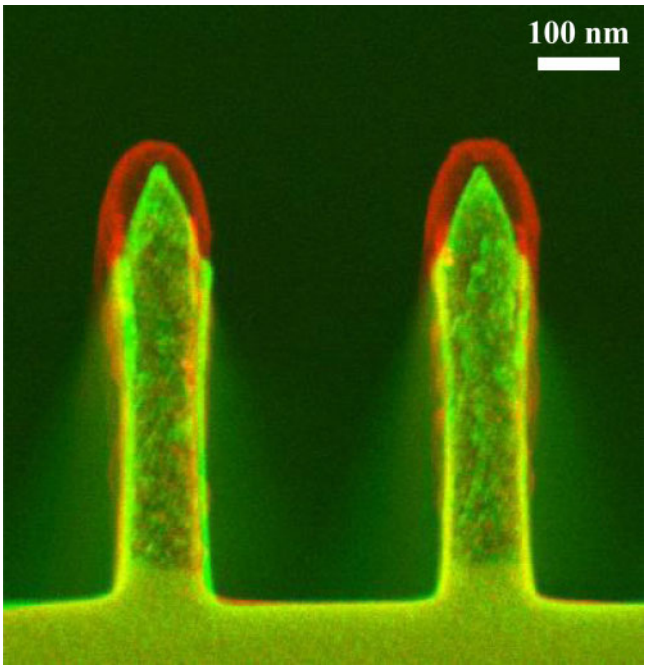

FIG. 10. False color overlay of Fig. 9(a) (yellow, green tone) and Fig. 9(b) (red tone) highlighting differences between the two SEM images. Nylon 6,2 MLD was preferentially located on top of the aC lines. No noticeable polymer MLD was observed in SiO_2 trenches. MLD on sidewalls of aC patterns was restricted due to sputtering and redeposition of SiO_2 on sidewalls during previous RIE.

isolating SiO_2 material during SEM imaging. Only the top of the aC lines was free from this SiO_2 redeposition.

Figure 9(b) shows the same test features after applying the H_2O_2 cleaning and DMA-TMS passivation pretreatments followed by 150 ED/AC MLD cycles at 125 °C. These 150 MLD cycles deposited ~20 nm of the nylon 6,2 polymer, located preferentially at the top of the aC lines. Using top-view CD SEM, the initial line CD of 125 nm was increased by adding ~16 nm of polymer to yield a line CD of 141 nm at the top after area-selective MLD.

Figure 10 displays an overlay of the cross-sectional SEM micrographs in Figs. 9(a) and 9(b), highlighting respective differences in false color. This overlay clarified that the nylon 6,2 MLD nucleated and grew preferentially at the top of the aC lines. These polymer deposits at the top of the aC lines were round and "mushroom-like." On the other hand, no noticeable polymer MLD was found on the SiO_2 trenches. This observation was confirmed by top-view SEM. Only minor, uneven polymer MLD was observed on the sidewalls of the aC lines. These sidewalls were believed to be coated in the RIE process by sputtered and redeposited SiO_2.

This area selectivity demonstrated in the overlay image for aC and SiO_2 in close proximity was consistent with the iSE results on individual, planar substrates. Nylon 6,2 MLD was selectively deposited on the aC surface area but not on passivated SiO_2 surface areas. Future optimization of the RIE process will attempt to prevent the sputtering and redeposition of SiO_2 on the sidewalls of the aC lines. After this optimization, area-selective polymer MLD should display its full potential for the maintenance of line CD. A variety of other polyamides[21–24] besides nylon 6,2 may be tested for area-selective MLD. Different polyamides may have varying degrees of resistance to RIE erosion.

Beyond the repair of aC hard masks used for pattern transfer, area-selective MLD may become important for the self-aligning growth of organic materials. Self-alignment will enable novel "bottom-up" nanomanufacturing schemes with a reduced number of processing steps.[57–59,64–66] This approach will be especially important for maskless processing that will eliminate conventional photolithography. Area-selective processing will provide an important advancement for reducing minimum feature sizes and for avoiding edge placement errors. In particular, area-selective MLD should enable a lithography-free, self-aligning formation of carbonaceous blocking layers for the fabrication of three-dimensional device structures.

IV. CONCLUSIONS

A method for the area-selective MLD of an all-organic polyamide was presented for deposition on aC surfaces and no deposition on SiO_2 surfaces. The polyamide MLD produced nylon 6,2 using alternating exposures of ED and AC. Surface cleaning, SiO_2 passivation, and nylon 6,2 MLD growth on various substrates was monitored by iSE. The area-selective deposition of nylon 6,2 MLD on three-dimensional test features with aC hard mask patterns and trenches in SiO_2 was characterized by SEM.

The nylon 6,2 film thickness incremented linearly around 1.6 Å per MLD cycle at 125 °C in the homogeneous, steady-state growth regime. The initiation of nylon 6,2 MLD was also monitored on a mildly oxidized aC surface and on a hydroxylated SiO_2 surface. The nylon 6,2 MLD nucleated and grew without delay on both surfaces. In contrast, passivation of the hydroxylated SiO_2 surface by selective, self-catalyzed chemisorption of DMA-TMS inhibited the nylon 6,2 MLD. A single passivation treatment with DMA-TMS converted the hydroxylated SiO_2 surface to an SiO_2 surface methylated with $-Si(CH_3)_3$ species. The methyl blocking layer remained intact for at least 100 MLD cycles and greatly restricted nylon 6,2 MLD on SiO_2. In contrast, the DMA-TMS treatment did not impact the MLD nucleation and growth on the aC surface.

After surface cleaning using H_2O_2 and then DMA-TMS exposures to passivate the SiO_2 surface, area-selective MLD produced at least 16 nm of a nylon 6,2 film on the aC "growth" surface with negligible deposition on the SiO_2 "nongrowth" surface. The area-selective MLD achieved an exceptionally high selectivity index above 98% for at least 100 MLD cycles. Etching of the scattered polymer deposits from the SiO_2 surface with O_3 or H_2O_2 was expected to result in even higher selectivity for an indefinite number of MLD cycles.

The area-selective MLD of nylon 6,2 was further demonstrated using trenches in SiO_2 fabricated by directional RIE through aC hard mask patterns. Cross-sectional and top-view SEM imaging of these three-dimensional test features revealed that the nylon 6,2 MLD grew selectively at the top of the aC patterns with no visible deposition on the underlying SiO_2 trench structures. The sidewalls

of the aC hard mask patterns were repellent to MLD because of redeposited SiO_2 on the sidewalls. Area-selective MLD of nylon 6,2 was demonstrated with great potential to maintain the critical dimension of aC hard masks by replacing carbonaceous material that is eroded during RIE.

ACKNOWLEDGMENTS

This work was funded by the Semiconductor Research Corporation (Task ID 2871.001). TEL is acknowledged for providing wafers with aC hard masks and various Si-based materials, for providing wafers with three-dimensional test features, as well as for SEM imaging. The authors also thank their industry liaisons, who provided valuable discussions and feedback in monthly telephone conferences: Eric C. Mattson, Charles C. Mokhtarzadeh, Jiun-Ruey Chen, Scott Clendenning (Intel); Robert D. Clark, Shigeru Tahara, Kanda Tapily, Omid Zandi, Angélique Raley, Christopher Cole (TEL); and Anuja De Silva (IBM).

REFERENCES

[1]S. K. Moore, IEEE Spectrum **56**, 9 (2019).
[2]G. Yeap *et al.*, *IEEE International Electron Devices Meeting*, San Francisco, CA, 7–11 December 2019 (IEEE, New York, 2019), p. 36.7.1.
[3]A. P. Jacob, R. Xie, M. G. Sung, L. Liebmann, R. T. P. Lee, and B. Taylor, Int. J. High Speed Electron. Syst. **26**, 1740001 (2017).
[4]M. M. Waldrop, Nature **530**, 144 (2016).
[5]S. Greengard, Commun. ACM **63**, 10 (2020).
[6]N. G. Orji *et al.*, Nat. Electron. **1**, 532 (2018).
[7]N. Rana, Y. Zhang, T. Kagalwala, and T. Bailey, J. Micro/Nanolithog. MEMS MOEMS **13**, 041415 (2014).
[8]C. W. Kaanta *et al.*, *International IEEE Conference on VLSI Multilevel Interconnection*, Santa Clara, CA, 11–12 June 1991 (IEEE, New York, 1991), p. 144.
[9]S. F. Al-Sarawi, D. Abbott, and P. D. Franzon, IEEE Trans. Compon. Packag. Manuf. Technol. B **21**, 2 (1998).
[10]I. M. Elfadel and G. Fettweis, *3D Stacked Chips: From Emerging Processes to Heterogeneous Systems* (Springer, New York, 2016).
[11]H. Radamson, Y. Zhang, X. He, H. Cui, J. Li, J. Xiang, J. Liu, S. Gu, and G. Wang, Appl. Sci. **7**, 1047 (2017).
[12]M. Geissler and Y. Xia, Adv. Mater. **16**, 1249 (2004).
[13]L. Li, X. Liu, S. Pal, S. Wang, C. K. Ober, and E. P. Giannelis, Chem. Soc. Rev. **46**, 4855 (2017).
[14]H. Abe, M. Yoneda, and N. Fujiwara, Jpn. J. Appl. Phys. **47**, 1435 (2008).
[15]B. Wu, A. Kumar, and S. Pamarthy, J. Appl. Phys. **108**, 051101 (2010).
[16]M. Kakuchi, M. Hikita, and T. Tamamura, Appl. Phys. Lett. **48**, 835 (1986).
[17]S. Pauliac-Vaujour, P. Brianceau, C. Comboroure, and O. Faynot, Microelectron. Eng. **85**, 800 (2008).
[18]G. A. Antonelli *et al.*, ECS Trans. **35**, 701 (2019).
[19]A. De Silva *et al.*, J. Vac. Sci. Technol. B **34**, 06KG03 (2016).
[20]Y. R. Park, B. S. Kwon, C. Y. Jung, W. Heo, N. E. Lee, and J. W. Shon, Thin Solid Films **519**, 6755 (2011).
[21]Y. Du and S. M. George, J. Phys. Chem. C **111**, 8509 (2007).
[22]N. M. Adamczyk, A. A. Dameron, and S. M. George, Langmuir **24**, 2081 (2008).
[23]D. J. Higgs, J. W. DuMont, K. Sharma, and S. M. George, J. Vac. Sci. Technol. A **36**, 01A117 (2018).
[24]B. C. Welch, O. M. McIntee, A. B. Ode, B. B. McKenzie, A. R. Greenberg, V. M. Bright, and S. M. George, J. Vac. Sci. Technol. A **38**, 052409 (2020).
[25]M. Putkonen, J. Harjuoja, T. Sajavaara, and L. Niinisto, J. Mater. Chem. **17**, 664 (2007).
[26]H. Zhou, M. F. Toney, and S. F. Bent, Macromolecules **46**, 5638 (2013).
[27]C. Zhang, M. Vehkamäki, M. Pietikäinen, M. Leskelä, and M. Ritala, Chem. Mater. **32**, 5073 (2020).
[28]C. Prasittichai, H. Zhou, and S. F. Bent, ACS Appl. Mater. Interfaces **5**, 13391 (2013).
[29]F. S. M. Hashemi, C. Prasittichai, and S. F. Bent, J. Phys. Chem. C **118**, 10957 (2014).
[30]C. Prasittichai, K. L. Pickrahn, F. S. Hashemi, D. S. Bergsman, and S. F. Bent, ACS Appl. Mater. Interfaces **6**, 17831 (2014).
[31]R. G. Closser, D. S. Bergsman, L. Ruelas, F. S. M. Hashemi, and S. F. Bent, J. Vac. Sci. Technol. A **35**, 031509 (2017).
[32]J. W. Elam, M. D. Groner, and S. M. George, Rev. Sci. Instrum. **73**, 2981 (2002).
[33]J. W. Klaus, O. Sneh, and S. M. George, Science **278**, 1934 (1997).
[34]J. W. Klaus and S. M. George, Surf. Sci. **447**, 81 (2000).
[35]J. D. Ferguson, E. R. Smith, A. W. Weimer, and S. M. George, J. Electrochem. Soc. **151**, G528 (2004).
[36]Y. Du, X. Du, and S. M. George, Thin Solid Films **491**, 43 (2005).
[37]Y. Du, X. Du, and S. M. George, J. Phys. Chem. C **111**, 219 (2007).
[38]R. Khan *et al.*, Chem. Mater. **30**, 7603 (2018).
[39]J. N. Hilfiker, N. Singh, T. Tiwald, D. Convey, S. M. Smith, J. H. Baker, and H. G. Tompkins, Thin Solid Films **516**, 7979 (2008).
[40]A. J. M. Mackus, M. A. Verheijen, N. Leick, A. A. Bol, and W. M. M. Kessels, Chem. Mater. **25**, 1905 (2013).
[41]M. Junige, M. Loffler, M. Geidel, M. Albert, J. W. Bartha, E. Zschech, B. Rellinghaus, and W. F. V. Dorp, Nanotechnology **28**, 395301 (2017).
[42]D. B. Mawhinney and J. T. Yates, Carbon **39**, 1167 (2001).
[43]P. Brender, R. Gadiou, J. C. Rietsch, P. Fioux, J. Dentzer, A. Ponche, and C. Vix-Guterl, Anal. Chem. **84**, 2147 (2012).
[44]R. L. Puurunen and W. Vandervorst, J. Appl. Phys. **96**, 7686 (2004).
[45]O. Sneh and S. M. George, J. Phys. Chem. **99**, 4639 (1995).
[46]D. Seghete, R. A. Hall, B. Yoon, and S. M. George, Langmuir **26**, 19045 (2010).
[47]D. S. Bergsman, R. G. Closser, and S. F. Bent, Chem. Mater. **30**, 5087 (2018).
[48]B. Kalanyan, P. C. Lemaire, S. E. Atanasov, M. J. Ritz, and G. N. Parsons, Chem. Mater. **28**, 117 (2016).
[49]M. M. Kerrigan, J. P. Klesko, S. M. Rupich, C. L. Dezelah, R. K. Kanjolia, Y. J. Chabal, and C. H. Winter, J. Chem. Phys. **146**, 052813 (2017).
[50]E. V. Anslyn and D. A. Dougherty, *Modern Physical Chemistry* (University Science, Sausalito, CA, 2004).
[51]G. A. Parks, Chem. Rev. **65**, 177 (1965).
[52]J. Bachmann *et al.*, Angew. Chem. Int. Ed. **47**, 6177 (2008).
[53]D. Hiller *et al.*, J. Appl. Phys. **107**, 064314 (2010).
[54]C. F. Herrmann, F. W. DelRio, V. M. Bright, and S. M. George, J. Micromech. Microeng. **15**, 984 (2005).
[55]O. Nilsen, C. E. Mohn, A. Kjekshus, and H. Fjellvåg, J. Appl. Phys. **102**, 024906 (2007).
[56]W. L. Gladfelter, Chem. Mater. **5**, 1372 (1993).
[57]A. J. Mackus, A. A. Bol, and W. M. Kessels, Nanoscale **6**, 10941 (2014).
[58]G. N. Parsons and R. D. Clark, Chem. Mater. **32**, 4920 (2020).
[59]F. S. Minaye Hashemi, C. Prasittichai, and S. F. Bent, ACS Nano **9**, 8710 (2015).
[60]R. Vallat, R. Gassilloud, B. Eychenne, and C. Vallée, J. Vac. Sci. Technol. A **35**, 01B104 (2017).
[61]R. Vallat, R. Gassilloud, O. Salicio, K. El Hajjam, G. Molas, B. Pelissier, and C. Vallée, J. Vac. Sci. Technol. A **37**, 020918 (2019).
[62]S. K. Song, H. Saare, and G. N. Parsons, Chem. Mater. **31**, 4793 (2019).
[63]M. F. J. Vos, S. N. Chopra, M. A. Verheijen, J. G. Ekerdt, S. Agarwal, W. M. M. Kessels, and A. J. M. Mackus, Chem. Mater. **31**, 3878 (2019).
[64]A. J. M. Mackus, M. J. M. Merkx, and W. M. M. Kessels, Chem. Mater. **31**, 2 (2019).
[65]S. Jesse *et al.*, ACS Nano **10**, 5600 (2016).
[66]R. Clark, K. Tapily, K. H. Yu, T. Hakamata, S. Consiglio, D. O'Meara, C. Wajda, J. Smith, and G. Leusink, APL Mater. **6**, 058203 (2018).